MgB_2 superconductors with addition of ZrB_2 and different carbon sources

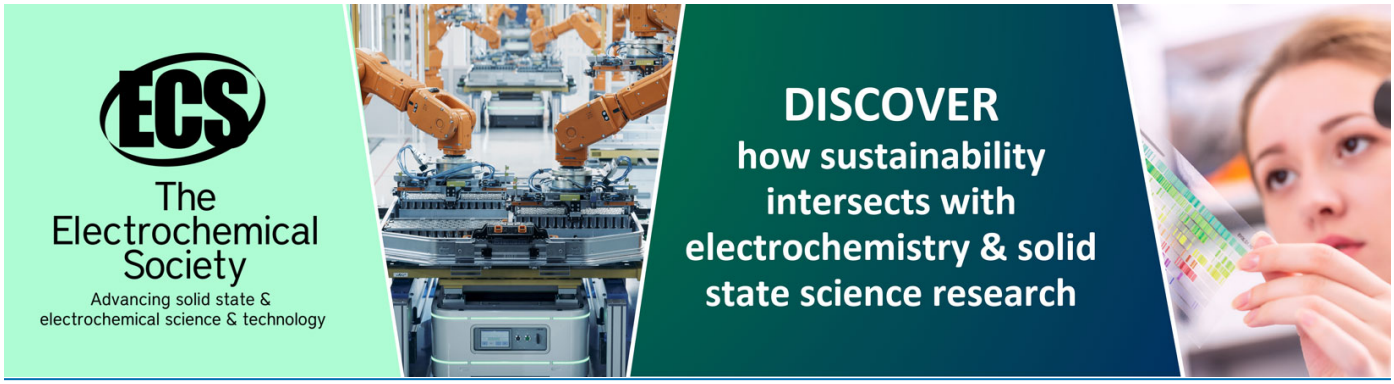

Journal of Physics: Conference Series **507** (2014) 012043 doi:10.1088/1742-6596/507/1/012043

MgB_2 superconductors with addition of ZrB_2 and different carbon sources

L B S Da Silva[1], E E Hellstrom[2], D Rodrigues Jr[1]

[1]Escola de Engenharia de Lorena, Universidade de São Paulo, Lorena, SP, Brazil.
[2]Applied Superconductivity Center, Florida State University, Tallahassee, FL, USA.

E-mail: lucasarno@usp.br, durval@demar.eel.usp.br

Abstract. MgB_2 has been catching the attention due to the possibility to apply the material in magnets and electronic devices, operating with cryocoolers. In this work, MgB_2 bulks were developed and analyzed with addition of ZrB_2, another diboride with the same C32 hexagonal structure as MgB_2, and simultaneous addition of different carbon sources (SiC, graphite, and carbon nanotubes). The objective of these additions is to modify the Mg planes with the diborides and to dope the material with carbon, improving the upper critical fields. Besides the doping of the material, this method creates crystalline defects in the superconducting matrix, which can act as pinning centers. As a result we could improve the critical current density of the material and estimate the behavior of dopants on the superconducting properties.

1. Introduction

Magnesium diboride (MgB_2) is one of the most promising superconductors for practical applications, due to its properties and characteristics, and to the low price of the precursor elements. The operation temperature of the application can be kept around 20K by cryocoolers. To reduce the problem with weak links and to improve the densification and intergrain connectivity in MgB_2, high energy ball-milling and hot isostatic pressing (HIP) have been used by research groups around the world [1,2].

The intensity that the magnetic flux lines are pinned in the MgB_2 defines the maximum critical current density (J_c) that the material can carry under a certain applied magnetic field (H). These pinning behaviors can be produced by defects in the superconducting matrix or other inhomogeneities in the material [3]. As MgB_2 is a granular material, the principal mechanism of flux pinning is due to the grain boundaries [4]. The processing scheme and the introduction of defects in the superconducting matrix can also influence the flux pinning efficiency and grain connectivity, simultaneously.

MgB_2 doping is another way to change the intrinsic superconducting properties, as the critical temperature (T_c) and upper critical magnetic field (B_{c2}). Research groups around the world have been investigating the doping of MgB_2 with different materials. Metallic elements, such as Li, Mn, Al, Ta, Zn, Cd, and others, are used to modify the Mg planes in the crystalline structure of the MgB_2. Carbon is one of the most effective element for significant enhancement of the critical current density at high magnetic fields, modifying the B planes [5,6]. The addition of materials with AlB_2–type crystalline structure (ZrB_2, TaB_2, VB_2, and AlB_2) has been investigated by our research group [1,5,7]. In these works, the addition of the diborides was efficient, changing the superconducting matrix, improving the magnetic flux pinning and, consequently, improving the transport properties of these superconductors. Simultaneous addition of diborides and carbon has not been systematically explored before [7].

In the present work a methodology to optimize J_c in bulks of MgB_2 superconductors is described. The method uses the addition of another diboride (ZrB_2) and simultaneous addition of a carbon source (SiC, graphite, and carbon nanotubes) to MgB_2 by high energy ball milling. The heat treatments were performed in a Hot Isostatic Press (HIP) to improve the densification and grain connectivity.

2. Experimental Procedure

MgB_2 samples were developed and analyzed with addition of ZrB_2 and simultaneous addition of carbon sources (SiC, graphite, and carbon nanotubes). The samples were prepared using pre-reacted Alfa-Aesar powders. The powder of MgB_2 was mixed to the ZrB_2 following the $Mg_{1-x}Zr_xB_2$ ratio, where x = 0.05 corresponds to the 5at.% concentration of the doping element. In some samples, 10wt.% of SiC, 3wt.% of graphite, and 3wt.% of carbon nanotubes (CNT) were added with the ZrB_2.

The mixing of the powders was performed with a SPEX 8000D high energy ball mill following the ball-to-powder mass ration of 3:1. All steps, including the preparation and mixture of the powders, were realized in a glove-box with argon atmosphere. The powders were compacted using a Cold Isostatic Press (CIP) under pressure of ~30 MPa. The heat treatments were performed in a Hot Isostatic Press (HIP), using slow heat-up with a 0.5°C/min rate to 1000ºC, heat treatment for 24h under a pressure of ~30 MPa, and slow cooling-down with a 0.2ºC/min rate to room temperature, to recrystallize and form the final phases, as well promoting the densification and the good intergrain connectivity. Table 1 shows the MgB_2 samples produced and analyzed in this work.

Table 1. Composition of the MgB_2 samples

Sample composition	Sample name
MgB_2	MgB_2
MgB_2+5at.%ZrB_2	ZrB_2
MgB_2+5at.%ZrB_2+10wt.%SiC	ZrB_2+SiC
MgB_2+5at.%ZrB_2+3wt.%graphite	ZrB_2+Graph
MgB_2+5at.%ZrB_2+3wt.%CNT	ZrB_2+CNT

X-ray diffractometry (XRD) was used to analyze the samples in an attempt to determine the formation of phases and the structural changes. The analysis were made using Cu-Kα X-ray radiation, scanning between 20º and 80º, and angular step of 0.02º in 2θ with 1s of counting per point, in a Shimadzu XRD-6000 Lab X diffractometer. The crystal structure refinements of all samples were performed from the X-ray diffractograms using the Rietveld method through the FullProf software (freeware). It was possible to extract an estimate of the sample's lattice parameters and composition.

The microstructural and compositional analysis of the samples after heat treatment were made using a scanning electron microscope (SEM) model LEO1450VP with an Oxford INCA energy dispersive spectrometer (EDS). The micrographs were obtained using a backscattered electrons detector. These analyses were important to verify the homogeneity, composition and granularity of the samples. A transmission electron microscope (TEM) model JEOL JEM2100 was used to complete the analysis.

The superconducting characterization was performed using a Quantum Design 9T PPMS. The critical temperatures T_c were extracted as the intersection point between the zero-field cooled (ZFC) and field cooled (FC) branches from the DC magnetization versus temperature curves measured under an applied magnetic field of 30 Oe. DC magnetization loops versus applied magnetic field at 5K were used to extract the $J_c(H,T=5K)$ *vs.* $\mu_0 H$ curves using the follow equation [8]:

$$J_c = \frac{20\Delta M}{a_1\left(1-\frac{a_1}{3a_2}\right)}; a_1 < a_2 \quad (1)$$

where ΔM is the difference of magnetization in a given field, a_1 and a_2 are the width and thickness, respectively, of the rectangular-shaped section extracted from the samples.

3. Results and Discussion

3.1. Crystallography Characterization

Table 2 is a compilation of results from X-ray analysis and the crystal structure refinement using the Rietveld method. All samples showed some MgO contamination and the formation of the MgB_4 phase, despite the careful sample preparation in all steps. The formation of the Mg_2Si phase can also be observed for samples with SiC additions. The formation of this phase can be explained by the Mg reaction with Si, which can be provided by the free Mg generated after its replacement by Zr in the crystalline structure. However, using conventional XRD analysis, there are no evidences of Mg replacement by Zr atoms. It is required a more accurate method to detect the doping. On the other hand, the significant decrease of the MgB_2 *a* lattice parameter indicates some carbon replacement at the boron sites of MgB_2, which is in agreement to the literature when using 10wt.% of SiC [6].

Table 2. Parameters obtained after Rietveld Refinement.

Sample	Phase	Composition (fract. %)	Lattice Parameters a (Å)	b (Å)	c (Å)
MgB_2	MgB_2	63.77	3.0835	3.0835	3.5216
	MgB_4	7.49	5.4543	4.3997	7.4745
	MgO	28.74	4.2138	4.2138	4.2138
ZrB_2	MgB_2	77.62	3.0817	3.0817	3.5259
	ZrB_2	21.24	3.1690	3.1690	3.5303
	MgB_4	0.57	5.6911	4.1949	7.5224
	MgO	0.56	4.2326	4.2326	4.2326
ZrB_2+SiC	MgB_2	44.99	3.0683	3.0683	3.5236
	ZrB_2	13.40	3.1649	3.1649	3.5260
	SiC	2.20	4.3508	4.3508	4.3508
	Mg_2Si	2.98	6.3551	6.3551	6.3551
	MgB_4	29.50	5.4643	4.4283	7.4723
	MgO	6.92	4.2176	4.2176	4.2176
ZrB_2+Graph	MgB_2	64.89	3.0639	3.0639	3.5254
	ZrB_2	19.97	3.1674	3.1674	3.5299
	MgB_4	6.45	5.6815	4.2039	7.5367
	MgO	8.69	4.2205	4.2205	4.2205
ZrB_2+CNT	MgB_2	61.21	3.0599	3.0599	3.5228
	ZrB_2	25.20	3.1669	3.1669	3.5285
	MgB_4	4.20	5.6866	4.2137	7.5739
	MgO	9.38	4.2138	4.2138	4.2138

3.2. Microstructural Characterization

Figure 1 presents the microstructure of the MgB_2 with addition of ZrB_2. The micrographs were obtained for the fractured surfaces by SEM analysis performed using the detector for backscattered electrons. The sample shows good connectivity, indicating that the preparation method and the heat treatment profile were efficient to create a dense MgB_2 superconducting phase. Some small clusters (light gray) were identified as ZrB_2 by EDS analysis. Figure 2 illustrates the TEM analysis of the ZrB_2 grains, which present an average grain size around 1 μm. Part of these secondary phases can act as pinning centers, improving the maximum J_c that the sample is capable to transport in the presence of an applied magnetic field. This effect will be even more pronounced if the secondary phase has dimensions in the order of the MgB_2 coherence length (less than 25nm), as reported in literature [9].

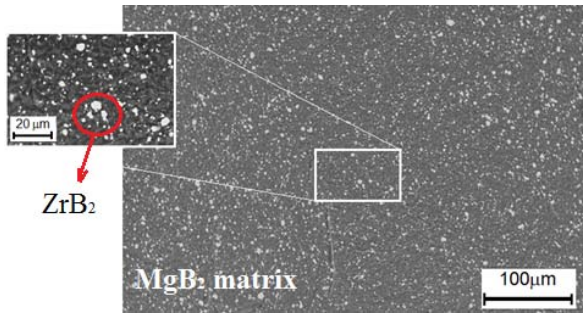

Figure 1. SEM analysis of the MgB_2 sample with ZrB_2 addition (ZrB_2), using backscattered electrons detection mode.

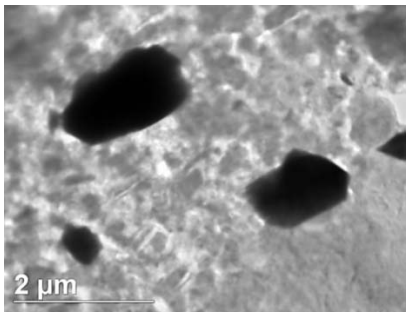

Figure 2. TEM analysis of the MgB_2 sample with ZrB_2 addition (ZrB_2). The grains of ZrB_2 are the dark regions and the light-gray is the MgB_2 matrix.

3.3. Analysis of the Superconducting Properties

Figure 3 shows the normal-to-superconductor transition using the ZFC and FC characterization. The critical temperatures T_c were extracted as the intersection point of the ZFC and FC curves. The pure MgB_2 sample showed T_c around 38.9 K. The critical temperature decreases to 38.2 K for the MgB_2 with ZrB_2 addition, and decreases to 36.2, 31.5, and 29.0 K for the MgB_2 samples with addition of SiC, graphite, and CNT, respectively. T_c decreases mainly due to changes in the MgB_2 matrix, which

is expected for doped samples. However, the values of T_c were maintained high for all samples and the transition widths were relatively narrow, showing the good quality of the superconducting phases.
Figure 4 shows the J_c vs. H curves for the MgB_2 samples at 5K. It can be seen that the samples with ZrB_2 addition showed improvements in J_c in the entire range of applied magnetic field, especially at low magnetic fields. This behavior can be probably explained by the creation of regions acting as effective pinning centers for the flux lines, like unreacted ZrB_2 or phases containing carbon.
On the other hand, simultaneous addition of ZrB_2 and graphite also presents an increase on J_c in the entire range of applied magnetic field, if compared with the pure MgB_2 sample, but more pronounced in high magnetic fields at 5K. The effective doping of the MgB_2 superconducting phase with carbon, as evidenced by the XRD analysis, is probably due to the replacement of boron by carbon in the MgB_2 crystalline structure. This behavior was already reported in the literature for samples mixed with a carbon source [6].

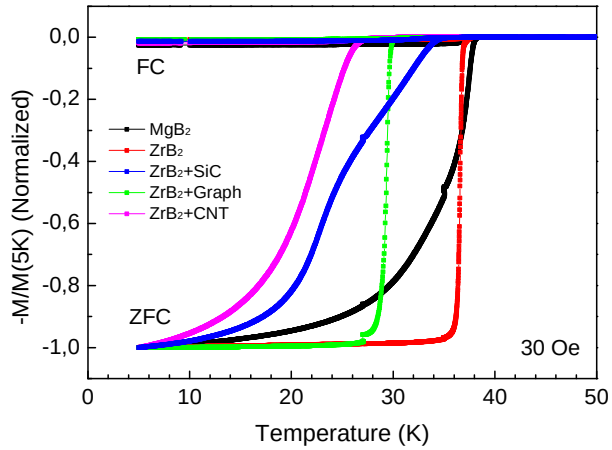

Figure 3. Normalized DC magnetization as a function of the temperature for MgB_2 samples, measured under 30 Oe.

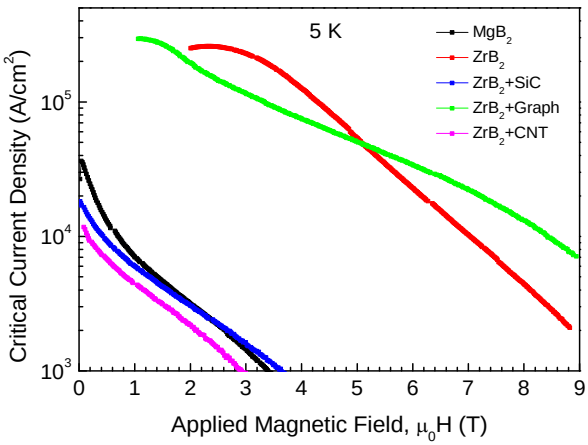

Figure 4. Critical current density as a function of the applied magnetic field for MgB_2 samples, measured at 5 K.

4. Conclusion

This work showed the results and a preliminary discussion of the possible reasons for the improvement of the transport properties of MgB_2 superconducting bulks when other diboride (ZrB_2) and carbon sources are added into the material. The additions of ZrB_2 and ZrB_2+graphite were efficient to improve J_c of the MgB_2 samples in all magnetic fields at 5 K. The combination of ZrB_2 and graphite showed the best transport conditions in high magnetic fields and at 5 K.

References

[1] Rodrigues Jr. D, Jiang J, Zhu Y, Voyles P, Larbalestier D C and Hellstrom E E 2009 *IEEE Trans. Appl. Supercond*. **19** 2797-2801.
[2] Serrano G, Serquis A, Dou S X, Soltanian S, Civale L, Maiorov B, Holesinger T G, Balakirev F and Jaime M 2008 *J. Appl. Phys*. **103** 023907.
[3] Da Silva L B S, Rodrigues C A, Oliveira Jr N F, Bormio-Nunes C and Rodrigues Jr D 2010 *Supercond. Sci. Technol.* **23** 115012.
[4] Buzea C and Yamashita T 2001*Supercond. Sci. Technol.* **14** R115-R146.
[5] Da Silva L B S, Rodrigues Jr D, Serrano G, Metzner V C V, Malachevsky M T and Serquis A 2011 *IEEE Trans. Appl. Supercond.* **21** 2639-2642.
[6] Dou S X, Pan A V, Zhou S, Ionescu S, Liu H K and Munroe P R 2002 *Supercond. Sci. Technol.* **15** 1587.
[7] Rodrigues Jr. D, Da Silva L B S, Metzner V C V and Hellstrom E E 2012 *Physics Procedia* **36** 468-474.
[8] Bean C P 1962 *Phys. Rev. Lett.* **8** 250.
[9] Mazin I I, Andersen O K, Jepsen O, Dolgov O V, Kortus J, Golubov A A, Kuz'menko A B and van der Marel D 2002 *Phys. Rev. Lett.* **89** 107002.